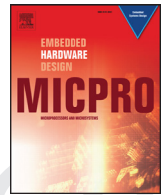




Contents lists available at ScienceDirect

Microprocessors and Microsystems

journal homepage: www.elsevier.com/locate/micpro

Exploiting antenna directivity in wireless NoC architectures

Q1 Andrea Mineo^{a,*}, Maurizio Palesi^b, Giuseppe Ascia^a, Vincenzo Catania^a^a University of Catania, ItalyQ2 ^b University of Enna, KORE, Italy

ARTICLE INFO

Article history:

Received 2 July 2015

Revised 25 January 2016

Accepted 29 January 2016

Available online xxx

Keywords:

Network-on-Chip

Wireless NoC

Energy efficiency

Antenna

ABSTRACT

Wireless Network-on-Chip (WiNoC) is an emerging on-chip communication paradigm and a candidate solution for dealing with the scalability problems which affect current and next generation many-core architectures. In a WiNoC, the transceivers that allow the conversion between electrical and radio signals, account for a significant fraction of the total communication energy budget. In particular, the transmitting power for wireless communications is strongly affected by the orientation of the antennas. This paper studies the impact of antennas orientation on energy figures of a WiNoC architecture and performs a design space exploration for determining the optimal orientation of the antennas in such a way to minimize the communication energy consumption. Experiments have been carried out on state-of-the-art WiNoC topologies, on both synthetic and real traffic scenarios, and validated by means of a commercial field solver simulator. When the antennas are optimally oriented, up to 80% energy saving (as compared to the case in which antennas have all the same orientation) has been observed.

© 2016 Elsevier B.V. All rights reserved.

1. Introduction

Accordingly to the predictions of the International Technology Roadmap for Semiconductors, the number of integrated processing elements into a modern multiprocessors system-on-chip (MPSoC) is increasing dramatically [1]. It is foreseen that the threshold of 1000 processing cores will be surpassed by the year 2020. A practical demonstration of such a trend can be observed by considering two prototypes developed by Intel [2,3]. The first one, developed in 2008, integrates 80 processing cores in a 65 nm CMOS technology, while the second one, developed after 5 years, integrates 256 cores in a 22 nm Tri-Gate CMOS technology. As the number of communicating cores increases, the role played by the on-chip communication system becomes more and more important. Both the above prototypes use a Network-on-Chip (NoC) as interconnection fabric. In fact, the NoC paradigm is considered as the most viable solution for addressing the communication issues in the context of many-core architectures [4].

Unfortunately, due to their multi-hop nature, as the network size increases, conventional NoCs which use electric point-to-point links, start to suffer from scalability problems, both in terms of communication latency and energy. For facing with such scalability

issues, several emerging interconnect paradigms such as Optical, 3D, and RF solutions have been proposed [5]. In particular, a specific class of RF interconnect introduces a wireless backbone upon traditional wire-based NoC substrate [6].

The use of the radio medium for on-chip communication is enabled by means of antennas and transceivers which form the core of a *radio-hub*. A radio-hub augments the communication capabilities of a conventional NoC switch/router by allowing it to wireless communicate with other radio-hubs in a single hop. The reduction of the average communication hop count, has a positive impact on both performance and power metrics but, the price to pay, regards the silicon area due for transceivers and antennas. Another aspect regards the attenuation introduced by the wireless channel. Since electromagnetic waves are propagated in lossy silicon, the power due to the wireless signaling represent an important contribution of the entire communication energy budget. In fact, in [7] it has been shown that the transmitter is responsible for about 65% of the overall transceiver power consumption, while in [8] such contribution is more than 74%. Thus, wireless communication results more energy efficient than wired communication when the communicating nodes are far away each other (in several studies such a distance has been reported being greater than two hops).

With regards to the amount of transmitting power needed to guarantee a certain reliability level (usually measured in terms of bit error rate), a common practice is computing the worst case attenuation and transmitting using such maximum power level irrespective of the location of the destination. Furthermore, in the

* Corresponding author. Tel.: +39 3493214359.

E-mail addresses: amineo@dieei.unict.it, andre.mineo@gmail.com (A. Mineo), maurizio.palesi@unikore.it (M. Palesi), giuseppe.ascia@dieei.unict.it (G. Ascia), vincenzo.catania@dieei.unict.it (V. Catania).

current WiNoC literature, the radiation pattern of the antenna is considered isotropic, that is, it is assumed that the antenna exhibits the same behavior irrespective of the transmitting/receiving directions. However, it is well known from antennas theory that the behavior of the antenna strongly depends on the direction from/to which the signal is received/transmitted. Such behavior is described by a fundamental antenna parameter, namely, *antenna directivity*, which describes the variation of the transmitting/receiving signal intensity for different observation angles. The directivity effects, widely studied in the context of free space communications, have been recently investigated in the context of intra-chip communications [9]. In the context of WiNoCs, however, there are no works in literature that take into account the directivity effects, and the antenna orientation is left out from the set of design parameters to be explored.

In this paper, we analyze the impact of antennas orientation on energy metrics in WiNoC architectures. Based on such analysis, we formulate the problem of finding the antennas orientation in such a way to minimize the total communication energy in the following two cases. The case in which the information about the applications that will be mapped on the WiNoC and their communication characteristics are not known, and the case in which they are known at design time. We refer to the first case as *general purpose* and the second one as *application specific*. Further, we also formulate the problem of finding the antennas orientation in such a way to minimize the transmitting power for the worst case. This latter problem is important in the case in which the WiNoC does not implement any technique for dynamic transmitting power calibration [10,11] and when the same transmitting power is used for any communicating pairs irrespective of their position into the WiNoC. Experiments, carried out on state-of-the-art WiNoC architecture, namely, HmWNoC [12] show that important energy saving, up to 80% can be obtained by properly set the orientation of the antennas.

2. Related work

The capability of MOS transistors of operating at frequencies as high as tens of GHz [13] makes it possible the development of fully integrated RF systems comprising integrated antennas and transceivers. In fact, as the frequency increases, dimensions of typical RF devices, such as antennas and inductors, decrease. For example, an antenna operating at 60 GHz can be as small as 680 μm in terms of axial length. Based on this, several research groups have experimentally proven the feasibility of inter- and intra-chip communication by using existing CMOS processes [9,14–16]. In particular, in the study conducted in [9], in which an experimental setup based on a test chip has been used, it has been shown that propagation mechanism in lossy silicon is based, mainly, on the propagation of surface waves. In the same work, the effects of metal structures and the contribution of antenna orientation has been investigated.

Wireless Network-on-Chip (WiNoC) paradigm has been recently proposed as a CMOS compatible solution [17] for addressing the scalability problems affecting the on-chip communication system for future many-core architectures. Several WiNoC architectures have been proposed in literature [12,18,19]. Since transceivers and antennas consume a relevant fraction of the total silicon area, in [12] the authors introduce several criteria to establish the optimum number of wireless interfaces under performance constraints. In the same work, a new architecture named *HmWNoC* has been presented. Such architecture exploits the *small-world* property [20] in which the network is divided in subnets and in which wireless and wire-line shortcuts can be used for inter-subnet communications. More recently, the same authors study the impact of various

modulation schemes in terms of silicon area and energy efficiency [19].

Other interesting WiNoC alternatives can be found in [21] and in [22]. In particular, the former proposes a wireless 3D NoC architecture which uses inductive coupling for inter-layer communication, while the latter introduces antennas based on graphene. Graphene-based antenna assures working frequency in the Terahertz band while utilizing lower chip area for antennas as compared to the metallic counterparts.

3. Background

Given a transmitting and a receiving antenna, this section provides the background on how computing the minimum transmitting power which guarantees a certain data rate and a maximum bit error rate (BER).

3.1. Signal strength requirements

For adapting the baseband signal to the wireless medium, the most used modulation scheme in the WiNoC context is Amplitude Shift Keying or On Off Keying (ASK-OOK) [12,18,19]. The reliability of the ASK-OOK modulation (in terms of BER) is related to the energy spent per bit, E_{bit} , as follows:

$$BER = Q\left(\sqrt{\frac{E_{bit}}{N_0}}\right), \quad (1)$$

where N_0 is the transceiver noise spectral density (noise introduced by the transceiver) and the Q function is the tail probability of the standard normal distribution which is defined in Eq. (2).

$$Q(x) = \frac{1}{\sqrt{2\pi}} \int_x^\infty e^{-\frac{y^2}{2}} dy \quad (2)$$

Since $E_{bit} = P_r/R_b$, where P_r is the power received at the terminal of the receiver antenna while R_b is the data rate, the required transmitting power for a given data rate and BER requirement and for a given transceiver's thermal noise can be computed as:

$$P_r = E_{bit} \cdot R_b = \left[Q^{-1}(BER)\right]^2 N_0 R_b, \quad (3)$$

where Q^{-1} is the inverse of the Q function. Thus, the minimum transmitting power needed for reaching the receiving antenna can be computed as:

$$P_t = P_r/G_a, \quad (4)$$

where, P_r is given by Eq. (3) and G_a is the attenuation introduced by the wireless medium ($G_a < 1$). The next subsection describes how the attenuation G_a can be computed.

3.2. Wireless medium attenuation

As discussed in the previous subsection, the required transmitting power depends on several factors, including, the type of modulation, the transceiver noise figure, and the attenuation introduced by the wireless medium. Let us consider Fig. 1 which shows a transmitting antenna with an output power P_t and a relative angle respect the receiving antenna of (θ_r, ϕ_r) , and a receiving antenna, located at distance R , with a relative angle respect the transmitting antenna of (θ_r, ϕ_r) . The fraction of the transmitting power that reaches the terminal of the receiving antenna, P_r , can be computed by means of the Friis transmission equation [23] valid when $R > 2D^2/\lambda$, where D is the maximum dimension of antenna (axial length in the considered case) and λ is the wavelength¹. The Friis

¹ For a zigzag antenna operating at 60 GHz, which has an axial length of 680 μm , the Friis equation is valid only if the distance R between two generic antennas is at least equal to $R_{MIN} = 0.18$ mm. The latter is obtained considering that in a silicon substrate the wavelength is about $\lambda = 5.02$ mm (in the range of millimeter waves).

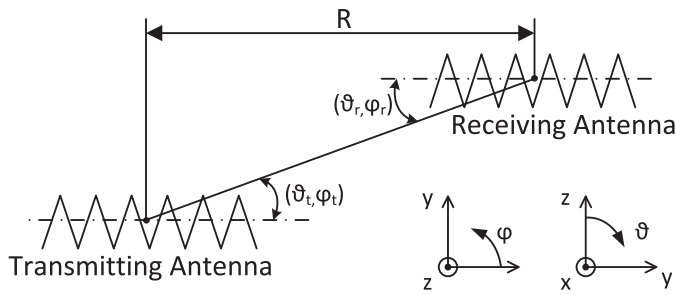


Fig. 1. Friis transmission equation: geometrical orientation of transmitting and receiving antennas. As indicated, considering a spherical coordinate system, ϕ is the azimuthal angle in the XY plane, where the X-axis is 0° and Y-axis is 90° . θ is the elevation angle where the Z-axis is 0° , and the XY plane is 90° .

158 transmission equation is:

$$G_a = \frac{P_r}{P_t} = e_t e_r \frac{\lambda^2 D_t(\theta_t, \phi_t) D_r(\theta_r, \phi_r)}{(4\pi R)^2}, \quad (5)$$

159 where:

- 160 • e_t and e_r are the efficiencies of the transmitting and receiving
161 antenna, respectively. These parameters mainly represent the
162 signal losses in the silicon substrate. For reducing such contribu-
163 tion, high resistivity Silicon on Insulator (SoI) substrates
164 ($> 1 \text{ K}\Omega\text{cm}$) can be used [24] or a polyamide stratus (few mic-
165 ron thick) can be inserted under the antenna [25].
- 166 • D_t and D_r are the directivities of the transmitting and receiv-
167 ing antenna, respectively. They quantify how much better the
168 antenna can transmit or receive in a specific direction.
- 169 • λ is the effective wavelength. For an IC substrate, it is estimated
170 by using the material properties of the top IC layers (silicon
171 dioxide $\epsilon_r = 3.9$) [26].

172 **Eq. (5)** highlights the parameters which determine the gain G_a
173 and represents a first order model of the wireless channel. In fact,
174 second order effects such as, polarization matching, wave reflec-
175 tions, and multi-path effects are not modeled by **Eq. (5)**. However,
176 in practical cases, G_a computation is estimated by means of **Eq. (6)**
177

$$G_a = \frac{P_r}{P_t} = \frac{|S_{12}|}{(1 - |S_{11}|)(1 - |S_{22}|)}, \quad (6)$$

178 where, S_{11} , S_{12} , and S_{22} are the scattering parameters. Such param-
179 eters are gathered by using field solver simulation tools [14] or by
180 direct measures from realized prototypes.

181 4. Antenna directivity optimization

182 4.1. Antenna directivity

183 As described by **Eq. (5)**, the attenuation introduced by the wire-
184 less medium, strongly depends on the directivity function. Based
185 on this, the orientation of the antennas in a WiNoC represents an
186 interesting parameter to be explored.

187 The energy consumed by a wireless communication between a
188 given transmitter and receiver pair, depends on their recipro-
189 cal location and orientations. Specifically, the energy consumed for
190 wirelessly transmitting a bit of information from transmitter i to
191 receiver j is:

$$E_{ij}^{tx} = \frac{P_{ij}}{\eta R_b}, \quad (7)$$

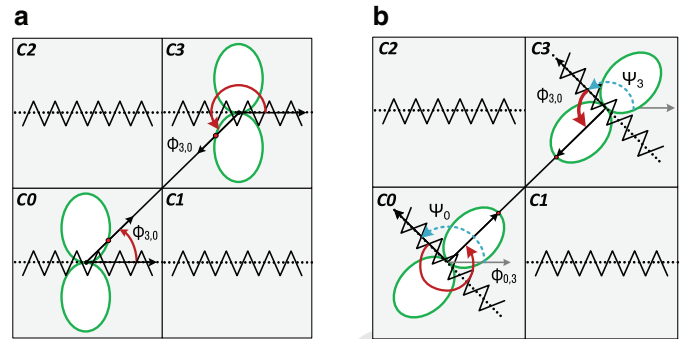


Fig. 2. Reciprocal antennas orientation and directivity functions. The directivity between C0 and C3 improves from configuration (a) to configuration (b).

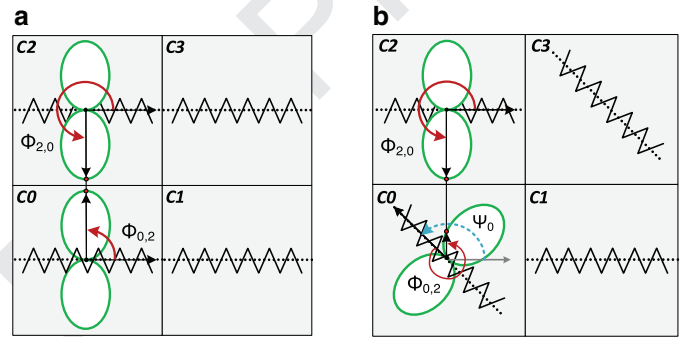


Fig. 3. Reciprocal antennas orientation and directivity functions. Configuration (a) improves communication energy between tiles C0 and C2 whereas configuration (b) improves communication energy between tiles C0 and C3.

where η is the transmitter efficiency. Considering **Eqs. (4)** and **(5)**,
the **Eq. (7)** can be written as:

$$E_{ij}^{tx} = \frac{P_r / D_t(\Phi_{ij}) D_r(\Phi_{ji}) \left(\frac{\lambda}{2\pi R_{ij}}\right)^2}{\eta R_b}. \quad (8)$$

Let ψ_i and ψ_j be a rotation of antenna i and antenna j as respect
to the die plane, respectively. Thus, **Eq. (8)** normalized by the con-
stant terms can be written as:

$$\overline{E}_{ij}^{tx} = \frac{R_{ij}^2}{D_t(\Phi_{ij} - \psi_i) D_r(\Phi_{ji} - \psi_j)}. \quad (9)$$

Thus, for minimizing the communication energy from i to j , it
needs to determine a rotation ψ_i and a rotation ψ_j such that
Eq. (9) is minimized.

For the sake of example, let us consider **Fig. 2(a)** in which four
antennas and their reciprocal orientations in the die plane are shown.
The energy consumption of the communication between tiles C0 and C3
can be minimized by maximizing the directivity of their respective
antennas. This is obtained by rotating the antennas in tiles C0 and C3
by the angles ψ_0 and ψ_3 , respectively, as shown in **Fig. 2(b)**.

It should be pointed out that, selecting a certain antenna orienta-
tion for improving the energy efficiency of a given transmitter/receiver
pair, might negatively affects the energy figures of other transmitter/receiver
pairs. For instance, the directivity of the antennas in tiles C0 and C2
before the rotation is maximized [see **Fig. 3(a)**] and thus, their commu-
nication energy is minimized. However, after the rotation of the anten-
nas in tiles C0 and C3 [see **Fig. 3(b)**], although the communication energy
between C0 and C3 improves, that between C0 and C2 worsens.

216 4.2. Formulation of the problem

217 Based on the above considerations, this subsection formulates
218 the problem of minimizing the wireless communication energy by
219 means of antennas orientation optimization. Specifically, three sce-
220 narios, namely, *application specific*, *general purpose*, and *worst case*
221 scenarios will be analyzed.

222 4.2.1. Application specific scenario

223 In the *application specific scenario* it is assumed that communi-
224 cation traffic information is available at design time. Let V_{ij} be the
225 traffic volume (in bits) from radio hub i to radio hub j . Let $E_{ij}(\Psi)$
226 be the energy consumption for transmitting one bit from radio hub
227 i to radio hub j when the antennas are oriented based the orienta-
228 tion vector Ψ . The i th component of Ψ represents the orientation
229 of the antenna of radio hub i . $E_{ij}(\Psi)$ is computed by Eq. (9). The
230 total normalized wireless communication energy can be computed as:
231

$$E_{tot}^{(as)}(\Psi) = \sum_{i=0}^N \sum_{j=0}^N V_{ij} \times E_{ij}(\Psi). \quad (10)$$

232 Thus, the problem of minimizing the wireless communication en-
233 ergy, by means of antennas orientation optimization, for the appli-
234 cation specific scenario can be formulated as finding the antennas
235 orientation vector Ψ which minimizes $E_{tot}^{(as)}(\Psi)$.

236 4.2.2. General purpose scenario

237 In the *general purpose scenario* it is assumed that communi-
238 cation traffic information is not available at design time. Based on
239 this, the same traffic volume for each communicating pair is as-
240 sumed. The total wireless communication energy per bit can be
241 computed as:

$$E_{tot}^{(gp)}(\Psi) = \sum_{i=0}^N \sum_{j=0}^N E_{ij}(\Psi). \quad (11)$$

242 Thus, the problem of minimizing the wireless communication en-
243 ergy, by means of antennas orientation optimization, for the gen-
244 eral purpose scenario can be formulated as finding the antennas
245 orientation vector Ψ which minimizes $E_{tot}^{(gp)}(\Psi)$.

246 4.2.3. Worst case scenario

247 Please notice that, in the above two scenarios (*application spe-*
248 *cific* and *general purpose*), it is assumed that the transceiver im-
249 plements a transmitting power calibration technique (e.g., [10,11])
250 which allows the transmitting radio hub to use the minimum
251 transmitting power to reach the destination guaranteeing a certain
252 bit error rate.

253 In WiNoCs in which the power amplifier (PA) in the transceivers
254 does not implement any transmitting power modulation mecha-
255 nism, the PA is configured to use the maximum transmitting power
256 irrespective of the recipient of the transmission. We refer to this
257 case as *worst case scenario*. In this case, the total wireless energy
258 consumption per bit is determined by the maximum $E_{ij}(\Psi)$:

$$E_{tot}^{(wc)}(\Psi) = \max_{i,j=1,\dots,N} E_{ij}(\Psi). \quad (12)$$

259 Thus, the problem of minimizing the wireless communication en-
260 ergy, by means of antennas orientation optimization, for the worst
261 case scenario can be formulated as finding the antennas orienta-
262 tion vector Ψ which minimizes $E_{tot}^{(wc)}(\Psi)$.

263 4.3. General design flow

264 The Friis equation used in the problem formulation is not suit-
265 able for computing the actual attenuation of the wireless medium.

In fact, it models only first order effects which are however enough
for early design space exploration. Thus, the use of accurate field
solver simulators or direct measurements on real prototypes are
needed for implement the overall optimization flow. The basic
steps which form the design flow can be summarized as follows.

1. Compute the radiation pattern of the antenna by means of a
field solver simulator or by test-chip measurements. The radi-
ation pattern represents the term D in Eq. (8).
2. Explore the antennas orientations design space for determining
the optimal antennas orientations which minimize the total
communication energy (cf., Subsection 4.2).
3. Configure the antennas with the orientations found in the pre-
vious step and compute the actual attenuation by means of a
field solver simulators for determining the transmitting power
for each antennas pair. Let $P_{i,j}$ be the transmitting power for
communication from antenna i to antenna j .
4. For the general purpose and application specific scenarios, use
the $P_{i,j}$ computed in the previous step for configuring the
variable gain amplifier controller [10,11]. For the worst case
scenario, set the transmitting power of every transmitter to
 $\max P_{i,j}$.
5. After that the antenna shapes has been drawn by means of a
standard layout CAD tool (selecting a specific metal layer), ap-
ply a rotation of the drawn objects in accordance with the op-
timization results.

In the next section, such design flow is applied for designing
energy efficient WiNoC configurations for the different scenarios,
under different traffic patterns and different parameters.

294 5. Experimental results

In this section we explore the design space spanned by the ori-
entations of the antennas in a WiNoC architecture with the goal of
improving its energy efficiency.

298 5.1. Simulation methodology

Given the non-linear, high dimensional, multi-modal, and non-
smooth nature of $E_{ij}(\Psi)$, the optimization problems Eqs. (13)–(15),
defined in the previous section, have been solved by means of sim-
ulated annealing.

$$\min_{\Psi} \sum_{i=0}^N \sum_{j=0}^N V_{ij} \times E_{ij}(\Psi) \quad (13)$$

$$\min_{\Psi} \sum_{i=0}^N \sum_{j=0}^N E_{ij}(\Psi) \quad (14)$$

$$\min_{\Psi} \max_{i,j=1,\dots,N} E_{ij}(\Psi) \quad (15)$$

Specifically, we have chosen the geometric annealing schedule [27]
as it is the most used and recommended one. The geometric an-
nealing temperature schedule defines the temperature at iteration
 i as $T = T_0 q^{L \cdot i}$, where T_0 is the initial temperature and L is the
number of iterations per temperature level and q is the geomet-
ric progression ratio to 0.9. In the experiments, the initial and final
temperatures have been set to 1 and 0.001, respectively. The maxi-
mum number of iterations, L , is set to $(N \times |\Psi|)^2$. The antenna ori-
entations are randomly generated, from the current configuration,
by interchanging two antennas, or by modifying the orientation of
an antenna.

For each of the above scenarios, namely, *application specific*
AS, Eq. (13), *general purpose GP*, Eq. (14), and *worst case WC*,

Table 1
HFSS setup parameters.

Parameter	Value
Chip size	20 mm × 20 mm
Technology	28 nm ² SOI
Silicon resistivity	$\rho = 5 \text{ K}\Omega\text{cm}$
Substrate thickness	350 μm
Oxide (SiO ₂) thickness	30 μm
Antenna elevation	2 μm
Antenna thickness	2 μm
Antenna axial length	2 × 340 μm
Operation frequency	60 GHz
Absolute bandwidth	16 GHz

Eq. (15), the optimal set of antennas orientation, namely, $\Psi_{opt}^{(AS)}$, $\Psi_{opt}^{(GP)}$, and $\Psi_{opt}^{(WC)}$, are simulated by means of an accurate field solver simulator for obtaining the scattering parameters. Then, scattering parameters are used by Eq. (6) for computing the transmitting power for each transmit–receive antenna pair. Such transmitting power data are then used for back-annotating a cycle accurate WiNoC simulator [28] for determining the total energy figures under different traffic scenarios.

In all the experiments we consider a zigzag antenna modeled and characterized with Ansoft HFSS [29] (High Frequency Structural Simulator). HFSS produces scattering parameter and radiation pattern as output. Table 1 reports the simulation parameters used in all the experiments. The selection of the chip size has been carried out in accordance with the International Technology Roadmap for Semiconductors (ITRS) [30] predictions on high-end MPSoCs.

Fig. 4 shows the antenna directivity, by means of its radiation pattern, considering the direction of maximum radiation under the substrate ($\phi = 100^\circ$).

5.2. Energy saving analysis

Let us know analyze the energy savings in the application specific (AS), general purpose (GP), and worst case (WC) scenarios. As communication traffic patterns, we used a set of representative applications of SPLASH-2 and PARSEC benchmarks suites. Such benchmarks have been executed on Graphite Multi-core Simulator [31] and the communication topology graphs and communication volumes information have been extracted. In all the experiments, the baseline WiNoC architecture is msWiNoC [12] in which all the antennas have the same orientation. In the case of AS and GP, it is assumed that the power amplifier in the transceivers is equipped with the reconfigurable variable gain amplifier (R-VGA) module [10] with seven power steps. The estimated transmitting power ranges from 8 μW (−21 dBm) to 794 μW (−1 dBm), that in terms of energy per bit correspond to 0.42 pJ/bit and 1.4 pJ/bit, respectively. Based on this, we have selected seven equally spaced power steps into such range. That is, the i th power step corresponds to a transmitting power of $8 + (i - 1) * 786/6 \mu\text{W}$.

Fig. 5 shows the percentage energy saving when the antennas are optimally oriented based on the solutions of optimization problems Eqs. (13)–(15) considering four antenna orientations steps. On average, up to 89%, 82%, and 78% energy saving is observed for AS, GP, and WC scenario, respectively.

Fig. 6 shows the percentage energy saving when the number of radio hubs is made to vary. As expected, the energy saving increases as the number of radio hubs increases due to the fact that more communications make use of the radio medium. However, no relevant improvement is observed when the number of radio hub is greater than eight. Such trend is related to the network size that in our experiments consists of 256 communicating cores. In fact, for such a medium network size, eight radio hubs are enough

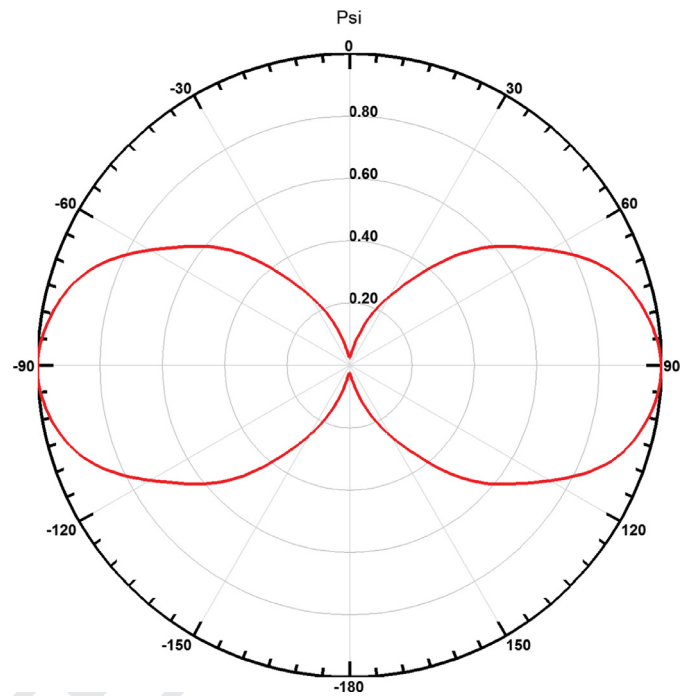


Fig. 4. Radiation pattern for a zigzag antenna at the elevation of maximum radiation ($\phi = 100^\circ$). $\theta = 0^\circ$ is the direction orthogonal to the antenna's main axis. According to Fig. 1, we assume the antenna situated upon the XY plane (coplanar with silicon die).

for drastically reducing the average hop count. Above eight radio hubs, the short distances between them, makes more suitable performing the communication by means of the wired underlying NoC. Please remind that, wireless transmissions becomes effective in term of energy efficiency when the path length is greater than three hops [8].

We analyzed four cases in which 2, 4, 8, and 16 orientations are allowed. Such allowed orientations are those obtained by equally dividing the orientations from 0° to 180° into 2, 4, 8, and 16 angles, respectively. Fig. 7 shows the percentage energy savings in such cases. It is interesting to observe that AS is quite insensitive to the increase of the number of admissible antenna orientations. This behavior is explained by the fact that AS directs the antenna along the direction with the maximum traffic volume. For this reason, having more than two available orientations, does not affect the solution found for AS. On contrary, GP and WC are strongly sensitive to the number of available antenna orientations. As it can be observed, passing from 2 to 4 possible orientations, it results in an energy saving gap of about 20% and 45% for GP and WC, respectively. For instance, in the case of GP, the optimal orientation of the antennas is determined by assuming that the traffic volume between all the radio hub pairs is the same. Thus, for a generic antenna, a trade-off orientation is determined in such a way to satisfy all the directions.

5.3. Case study

As a real case study, we consider a complex heterogeneous platform shown in Fig. 8. The system is composed by a generic MultiMedia System which includes a H.263 video encoder, a H.263 video decoder, a MP3 audio encoder and a MP3 audio decoder [32], a MIMO-OFDM receiver [33], a Picture-In-Picture application (PiP) [34] and a Multi-Window Display application (MWD) [35]. Fig. 8 shows the application mapped on a HmWNoC [12] partitioned in 16 subnetworks where the upper level network is a 2D mesh topology augmented with three radio hubs. The number of

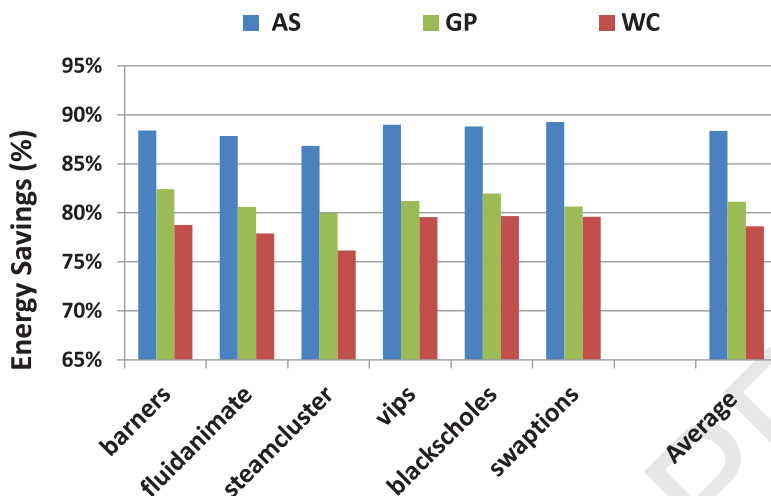


Fig. 5. Energy saving obtained for ms-WiNoC with 256 nodes under different traffic scenarios.

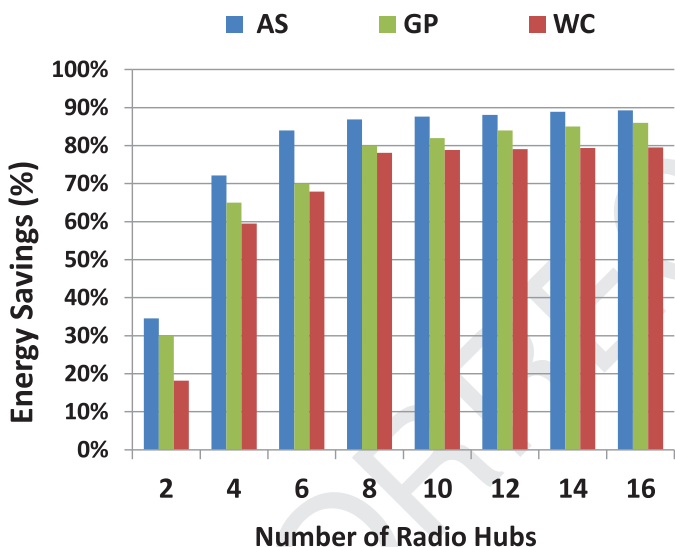


Fig. 6. Energy saving for different number of radio hubs.

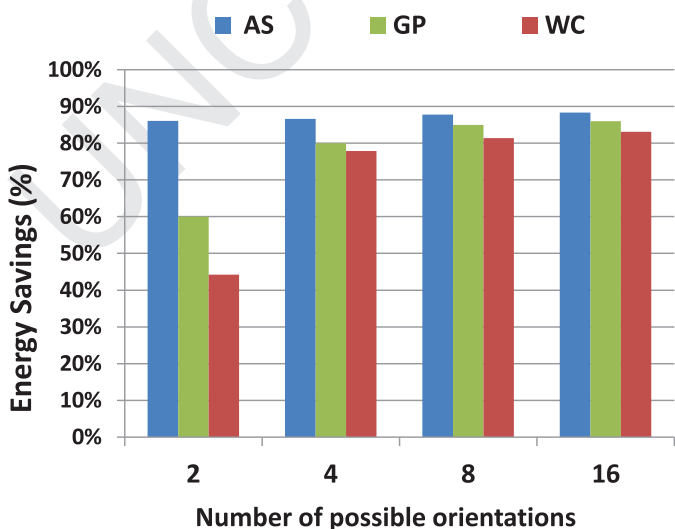


Fig. 7. Energy saving for various number of possible orientations of the antenna (WiNoC configured with 16 radio hubs).

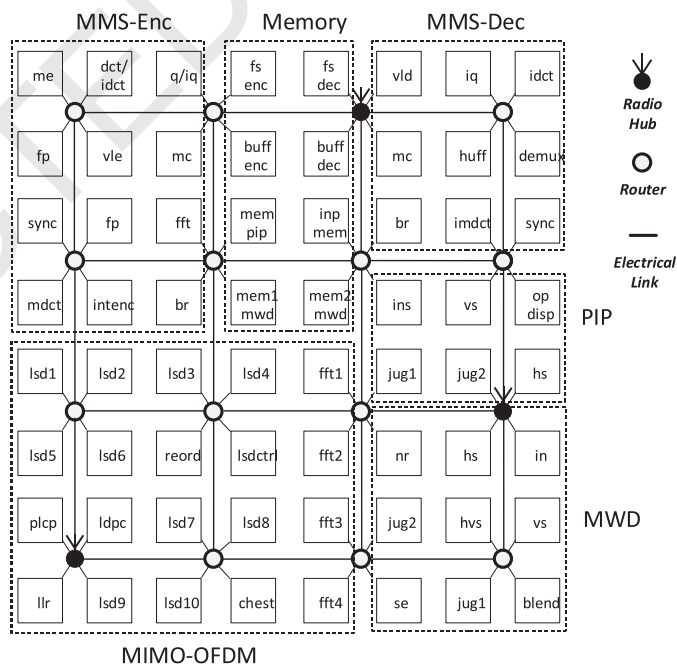


Fig. 8. Heterogeneous system composed by a multimedia sub-system, a MIMO-OFDM receiver, a PIP and a MWD module.

radio hubs and their placement into the network has been derived by using the optimization procedure described in [12].

We explore the antennas orientation design space for both the application specific (AS) and worst case (WC) scenarios. We consider antennas can be oriented among four angles (0°, 45°, 90°, 135°). We assume a tunable power amplifier supporting seven power steps with a transmitting energy per bit ranging from 0.42 pJ/bit to 1.4 pJ/bit. Fig. 9 shows the optimal orientation of the three antennas for the two scenarios. With regard to the AS scenario, due to the presence of memory elements close to C14, which represents an hot-spot region of the network, there is a relevant traffic volume between such region and both C0 and C7. Based on this, as can be observed from Fig. 9 (AS), both antennas in C7 and C0 are oriented in such a way to reduce energy when communicate with C14. With regard to the WC scenario, since no traffic information is used during the design space exploration, the optimal orientation of the antennas found, tries to minimize the

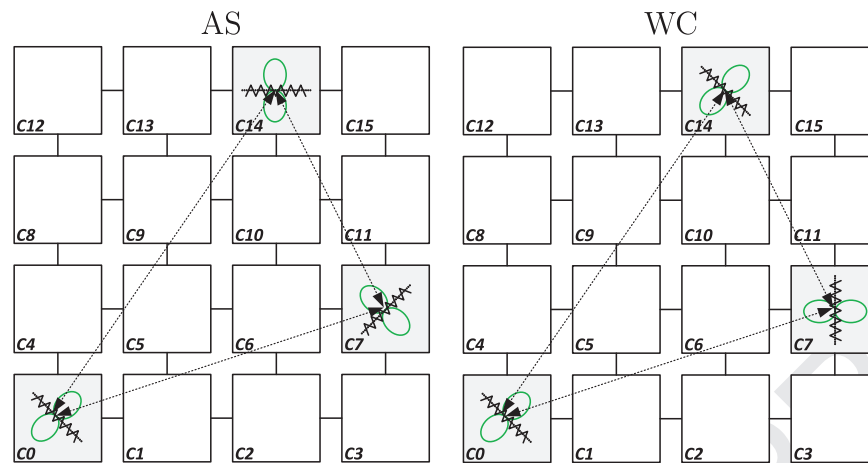


Fig. 9. Optimal antennas orientations found by the simulated annealing algorithm for the application specific (AS) and worst case (WC) scenarios.

Table 2

Transmitting energy per bit for each transmitting and receiving antennas pair.

TX	RX	Transm. energy (pJ/bit)		
		BS	AS	WC
C14	C7	1.40	0.58	1.07
C14	C0	1.40	1.23	1.07
C7	C14	1.40	0.58	1.07
C7	C0	1.40	0.91	1.07
C0	C14	1.40	1.23	1.07
C0	C7	1.40	0.91	1.07
Total energy (J)		1.68×10^{-4}	1.23×10^{-5}	1.02×10^{-4}

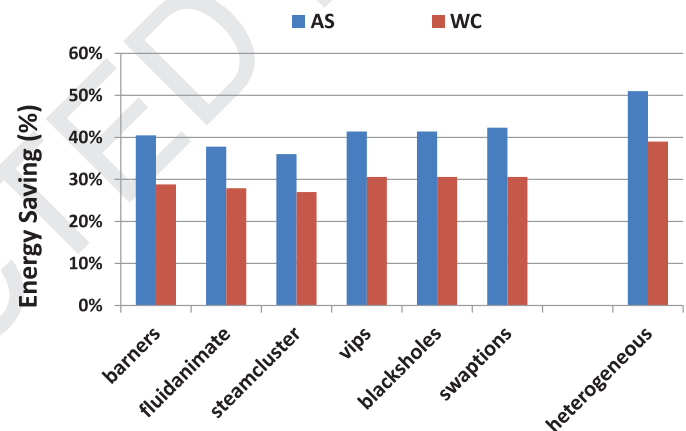


Fig. 10. Energy saving obtained for ms-WiNoC with 64 nodes under different traffic scenarios and for the heterogeneous platform of the case study.

418 worst case condition which is represented by the communication
 419 between the two far apart clusters, namely, C14 and C0. In fact, as
 420 it can be noticed, the antenna in C14 fits the directivity of the an-
 421 antenna in C0 and viceversa. This is due to the fact that, C0 is closer
 422 to C7 than C14. This scenario highlights, in fact, the importance of
 423 the distance R during the optimization process Eq. (9).

424 Table 2 reports, for each transmitting and receiving antennas
 425 pair, and for each considered scenario, the transmitting energy per
 426 bit. The table also shows a baseline scenario (BS) in which all the
 427 antennas have the same orientation (0°). Of course, for both the
 428 WC and BS scenarios, the transmitting energy is constant irrespec-
 429 tive of the location of the transmitting and receiving antenna. The
 430 optimization of the antennas orientation in the WC scenario allows
 431 to reduce the communication energy by 39% as respect to the BS
 432 scenario. By considering the AS scenario, in which the transmitting
 433 power is tuned online, the communication energy reduces by 51%.

434 Please notice that, the energy saving figures obtained for the
 435 heterogeneous multimedia system, although they seem to be
 436 aligned with those found for the typical parallel applications (i.e.,
 437 SPLASH-2 and PARSEC), they are actually more relevant. In fact,
 438 the heterogeneous multimedia system is mapped on a 64-core NoC
 439 whereas the general parallel applications have been assessed on a
 440 256-core NoC. For a more fair comparison, the same experiment,
 441 whose results have been shown in Fig. 5, has been repeated on
 442 a 64-node NoC and the obtained energy savings are shown in
 443 Fig. 10. As it can be observed, on average, the energy saving is
 444 29% and 40% for the WC and AS scenarios, respectively, which is
 445 more than 10% less energy efficient of what has been observed for
 446 the heterogeneous case study. The higher energy saving obtained
 447 for the heterogeneous system is justified by the less uniformity
 448 of the communication patterns which characterizes heterogeneous
 449 systems and that are exploited by the proposed technique.

6. Conclusions

451 In a WiNoC the transceivers of the radio hubs account for a
 452 significant fraction of the total communication energy budget.
 453 Several work in literature in the context of low power WiNoC
 454 architectures, do not take into account the impact of the antenna
 455 directivity on power metrics. In addition, they assume that anten-
 456 nas present an omnidirectional radiation pattern which is far away
 457 from the reality (see, for instance, Fig. 4). In this paper we have
 458 highlighted the need for antennas orientation design space explo-
 459 ration for improving the energy figures of WiNoC architectures. We
 460 have considered three main scenarios, namely, application specific
 461 (AS), general purpose (GP), and worst case (WC). In the AS sce-
 462 nario, communication information are exploited for optimizing the
 463 orientation of the antennas in such a way to maximize the overlap
 464 of the radiation patterns of the antennas which communicate
 465 more. The GP scenario, is derived from AS by assuming that all the
 466 radio hubs communicate each other with the same probability. Fi-
 467 nally, the WC scenario is when the transceiver does not implement
 468 any transmitting power on-line calibration scheme and, therefore,
 469 all the radio hubs communicate using the same transmitting power
 470 irrespective of their location in the chip. A state of the art small-
 471 world based WiNoC architecture has been used as reference WiNoC
 472 architecture in the experiments. The exploration of the antennas
 473 orientation design space under different traffic patterns resulted
 474 in important energy savings in all the three scenarios considered.

475 References

- 476 [1] ITRS 2011 edition - system drivers, 2011, (International Technology Roadmap
477 for Semiconductors).
- 478 [2] S.R. Vangal, J. Howard, G. Ruhl, S. Dighe, H. Wilson, J. Tschanz, D. Finan,
479 A. Singh, T. Jacob, S. Jain, V. Erraguntla, C. Roberts, Y. Hoskote, N. Borkar,
480 S. Borkar, An 80-tile sub-100-W TeraFLOPS processor in 65-nm CMOS, IEEE
481 J. Solid State Circuits 43 (1) (2008) 29–41.
- 482 [3] G. Chen, M.A. Anders, H. Kaul, S.K. Satpathy, S.K. Mathew, S.K. Hsu, A. Agarwal,
483 R.K. Krishnamurthy, S. Borkar, V. De, 16.1 A 340mV-to-0.9V 20.2Tb/s Source-
484 synchronous Hybrid packet/circuit-switched 16x16 Network-on-Chip in 22nm
485 Tri-Gate CMOS, in: Solid-State Circuits Conference Digest of Technical Papers
486 (ISSCC), 2014 IEEE International, 2014, pp. 276–277, doi:10.1109/ISSCC.2014.
487 6757432.
- 488 [4] L. Benini, G.D. Micheli, Networks on chips: a new SoC paradigm, IEEE Comput.
489 35 (1) (2002) 70–78.
- 490 [5] L.P. Carloni, P. Pande, Y. Xie, Networks-on-chip in emerging interconnect
491 paradigms: Advantages and challenges, in: Networks-on-Chip, 2009. NoCS
492 2009. 3rd ACM/IEEE International Symposium on, 2009, pp. 93–102.
- 493 [6] S. Deb, A. Ganguly, P. Pande, B. Belzer, D. Heo, Wireless noc as interconnec-
494 tion backbone for multicore chips: Promises and challenges, Emerg. Sel. Top.
495 Circuits Syst., IEEE J. 2 (2) (2012) 228–239, doi:10.1109/JETCAS.2012.2193835.
- 496 [7] X. Yu, S. Sah, S. Deb, P. Pande, B. Belzer, D. Heo, A wideband body-enabled
497 millimeter-wave transceiver for wireless network-on-chip, in: Circuits and Sys-
498 tems (MWSCAS), 2011 IEEE 54th International Midwest Symposium on, 2011,
499 pp. 1–4, doi:10.1109/MWSCAS.2011.6026282.
- 500 [8] D. Daly, A. Chandrakasan, An energy-efficient oook transceiver for wireless sen-
501 sor networks, Solid State Circuits IEEE J. 42 (5) (2007) 1003–1011, doi:10.1109/
502 JSSC.2007.894323.
- 503 [9] Y.P. Zhang, Z.M. Chen, M. Sun, Propagation mechanisms of radio waves over
504 intra-chip channels with integrated antennas: Frequency-domain measure-
505 ments and time-domain analysis, Antennas Propag. IEEE Trans. 55 (10) (2007)
506 2900–2906, doi:10.1109/TAP.2007.905867.
- 507 [10] A. Mineo, M. Palesi, G. Ascia, V. Catania, An adaptive transmitting power tech-
508 nique for energy efficient mm-wave wireless nocs, in: Design, Automation Test
509 in Europe Conference (DATE14), 2014.
- 510 [11] A. Mineo, M.S. Rusli, M. Palesi, G. Ascia, V. Catania, M.N. Marsono, A closed
511 loop transmitting power self-calibration scheme for energy efficient winoc ar-
512 chitectures, in: To be appear in Design, Automation Test in Europe Conference
513 (DATE15), 2015.
- 514 [12] S. Deb, K. Chang, X. Yu, S. Sah, M. Cosic, A. Ganguly, P. Pande, B. Belzer,
515 D. Heo, Design of an energy-efficient cmos-compatible noc architecture with
516 millimeter-wave wireless interconnects, Comput. IEEE Trans. 62 (12) (2013)
517 2382–2396.
- 518 [13] ITRS 2012 update - rf and analog/mixed-signal technologies (rfams), 2012, (In-
519 ternational Technology Roadmap for Semiconductors).
- 520 [14] B. Floyd, C.-M. Hung, K. O. Intra-chip wireless interconnect for clock distribu-
521 tion implemented with integrated antennas, receivers, and transmitters, Solid
522 State Circuits IEEE J. 37 (5) (2002) 543–552, doi:10.1109/4.997846.
- 523 [15] J. Lin, H.-T. Wu, Y. Su, L. Gao, A. Sugavanam, J. Brewer, K. O. Communication
524 using antennas fabricated in silicon integrated circuits, Solid State Circuits IEEE
525 J. 42 (8) (2007) 1678–1687, doi:10.1109/JSSC.2007.900236.
- 526 [16] X. Yu, S.P. Sah, Rashtian, H. Rashtian, S. Mirabbasi, P.P. Pande, D. Heo, A 1.2-
527 pj/bit 16-gb/s 60-ghz oook transmitter in 65-nm cmos for wireless network-on-
528 chip, Microw. Theory Tech. IEEE Trans. 62 (10) (2014) 2357–2369, doi:10.1109/
529 TMTT.2014.2347919.
- 530 [17] D. Zhao, Y. Wang, Sd-mac: design and synthesis of a hardware-efficient
531 collision-free qos-aware mac protocol for wireless network-on-chip, Comput.
532 IEEE Trans. 57 (9) (2008) 1230–1245, doi:10.1109/TC.2008.86.
- 533 [18] D. DiTomaso, A. Kodi, S. Kaya, D. Matolak, iwise: Inter-router wireless scal-
534 able express channels for network-on-chips (nocs) architecture, in: High Per-
535 formance Interconnects (HOTI), 2011 IEEE 19th Annual Symposium on, 2011,
536 pp. 11–18, doi:10.1109/HOTI.2011.12.
- 537 [19] X. Yu, J. Baylon, P. Wettin, D. Heo, P.P. Pande, S. Mirabbasi, Architecture and
538 design of multi-channel millimeter-wave wireless network-on-chip, Des. Test
539 IEEE PP (99) (2014) 1–1, doi:10.1109/MDAT.2014.2322995.
- 540 [20] U. Ogras, R. Marculescu, "It's a small world after all": Noc performance opti-
541 mization via long-range link insertion, Very Large Scale Integr. (VLSI) Syst. IEEE
542 Trans. 14 (7) (2006) 693–706, doi:10.1109/TVLSI.2006.878263.
- 543 [21] Y. Take, H. Matsutani, D. Sasaki, M. Koibuchi, T. Kuroda, H. Amano, 3D NoC
544 with inductive-coupling links for building-block SiPs, Comput. IEEE Trans. 63
545 (3) (2014) 748–763, doi:10.1109/TC.2012.249.
- 546 [22] S. Abadal, E. Alarcón, A. Cabellos-Aparicio, M.C. Lemme, M. Nemirovsky,
547 Graphene-enabled wireless communication for massive multicore architec-
548 tures, Commun. Mag. IEEE 51 (11) (2013) 137–143, doi:10.1109/MCOM.2013.
549 6658665.
- 550 [23] C. Balanis, Modern Antenna Handbook, Wiley, 2008.
- 551 [24] S. Montusclat, F. Gianesello, D. Gloria, S. Tedjini, Silicon integrated antenna de-
552 velopments up to 80 ghz for millimeter wave wireless links, in: Wireless Tech-
553 nology, 2005. The European Conference on, 2005, pp. 237–240, doi:10.1109/
554 ECWT.2005.1617701.

- 555 [25] S.-B. Lee, S.-W. Tam, I. Pefkianakis, S. Lu, M.F. Chang, C. Guo, G. Reinman,
556 C. Peng, M. Naik, L. Zhang, J. Cong, A scalable micro wireless interconnect
557 structure for CMPs, in: Proceedings of the 15th annual international confer-
558 ence on Mobile computing and networking, in: MobiCom '09, ACM, New York,
559 NY, USA, 2009, pp. 217–228, doi:10.1145/1614320.1614345.
- 560 [26] F. Gutierrez, S. Agarwal, K. Parrish, T. Rappaport, On-chip integrated antenna
561 structures in cmos for 60 ghz wlan systems, Sel. Areas Commun. IEEE J. 27
562 (8) (2009) 1367–1378, doi:10.1109/JSA.2009.091007.
- 563 [27] D. Fouskakis, D. Draper, Stochastic optimization: a review, Int. Stat. Rev. 70 (3)
564 (2007) 315–349.
- 565 [28] F. Fazzino, M. Palesi, D. Patti, winoxim: Wireless Network-on-Chip simulator,
566 (<https://code.google.com/p/winoxim/>).
- 567 [29] Ansoft HFSS.
- 568 [30] ITRS, International technology roadmap for semiconductors.
- 569 [31] J.E. Miller, H. Kasture, G. Kurian, C.G. III, N. Beckmann, C. Celio, J. Eastep,
570 A. Agarwal, Graphite: A distributed parallel simulator for multicores, in: IEEE
571 International Symposium on High-Performance Computer Architecture, 2010.
- 572 [32] J. Hu, R. Marculescu, Energy- and performance-aware mapping for regular
573 NoC architectures, IEEE Trans. Comput. Aided Des. Integr. Circuits Syst. 24 (4)
574 (2005) 551–562.
- 575 [33] S.-R. Yoon, J. Lee, S.-C. Park, Case study: Noc based next-generation wlan re-
576 ceiver design in transaction level, in: International Conference on Advanced
577 Communication Technology, 2006, pp. 1125–1128.
- 578 [34] E.G.T. Jaspers, P.H.N. de With, Chip-set for video display of multimedia infor-
579 mation, IEEE Trans. Consum. Electron. 45 (3) (1999) 706–715.
- 580 [35] E.B. van der Tol, E.G. Jaspers, Mapping of MPEG-4 decoding on a flexible archi-
581 tecture platform, Media Process. 4674 (2002) 362–375.



Andrea Mineo received the BSc and MSc degrees in Elec-
tronic Engineering from the University of Catania, Italy,
in 2010 and 2013, respectively. Currently, he is PhD can-
didate in Systems, Energy, Computer and Telecommuni-
cations Engineering at the University of Catania. His re-
search interests include VLSI systems, Network-on-Chip
architectures and emerging interconnect technologies for
on-chip networks.



Maurizio Palesi received the M.Sc. degree and the Ph.D.
in Computer Science Engineering from the University of
Catania, Italy, in 1999 and 2003, respectively. He is an
Associate Professor with the Information Processing Sys-
tems, Kore University of Enna, Enna, Italy. He has pub-
lished one book, six book chapters, and over 110 refereed
international journals and conference papers. His current
research interests include embedded systems design and
singlechip implementations of complete embedded sys-
tems known as system-on-chip. Dr. Palesi was a recipi-
ent of the Best Paper Award from DATE 2011. He is an
Associate Editor of eight publications. He has served as a
Guest Editor for several international journals.



Giuseppe Ascia received the M.Sc. degree in Electronic
Engineering and the Ph.D. degree in Computer Science
from the University of Catania, Italy, in 1994 and 1998,
respectively. Since 1994, he has collaborated with the De-
partment of Electrical, Electronic and Computer Engin-
eering, University of Catania where he is currently an Asso-
ciate Professor of Computer Science and Engineering. His
current research interests include soft computing, very
large scale integration design, network-on-chip and low-
power design.



Vincenzo Catania received the Laurea degree in Electri-
cal Engineering from the University of Catania, Italy, in
1982. Until 1984, he was responsible for testing micro-
processor system at STMicroelectronics, Catania. He is a
full professor of computer science. His research interests
include performance and reliability assessment in paral-
lel and distributed system, VLSI design, low power design,
and fuzzy logic.